Gate controlled electronic transport in monolayer MoS$_2$ field effect transistor

Y. F. Zhou,[1] H. M. Xian,[2] B. Wang,[1] Y. J. Yu,[1] Y. D. Wei,[1,a)] and J. Wang[3,a)]

[1]*School of Physics Science and Technology, and Institute of Computational Condensed Matter Physics, Shenzhen University, Shenzhen 518060, People's Republic of China*
[2]*School of Physics and Optoelectronics, South China University of Technology, Guangzhou, People's Republic of China*
[3]*Department of Physics, The University of Hong Kong, Pokfulam Road, Hong Kong, People's Republic of China*

The electronic spin and valley transport properties of a monolayer MoS$_2$ are investigated using the non-equilibrium Green's function formalism combined with density functional theory. Due to the presence of strong Rashba spin orbit interaction (RSOI), the electronic valence bands of monolayer MoS$_2$ are split into spin up and spin down Zeeman-like texture near the two inequivalent vertices K and K' of the first Brillouin zone. When the gate voltage is applied in the scattering region, an additional strong RSOI is induced which generates an effective magnetic field. As a result, electron spin precession occurs along the effective magnetic field, which is controlled by the gate voltage. This, in turn, causes the oscillation of conductance as a function of the magnitude of the gate voltage and the length of the gate region. This current modulation due to the spin precession shows the essential feature of the long sought Datta-Das field effect transistor (FET). From our results, the oscillation periods for the gate voltage and gate length are found to be approximately 2.2 V and $20.03a_B$ (a_B is Bohr radius), respectively. These observations can be understood by a simple spin precessing model and indicate that the electron behaviors in monolayer MoS$_2$ FET are both spin and valley related and can easily be controlled by the gate. © *2015 AIP Publishing LLC.*
[http://dx.doi.org/10.1063/1.4914954]

I. INTRODUCTION

Recently, intense research efforts have been focused on the atomically thin two-dimensional (2D) materials such as graphene,[1–3] silicence,[4–6] and two dimensional (2D) transition metal dichalcogenides (TMDCs).[7–15] Bulk TMDCs, which are denoted as MX$_2$ with M = Mo or W and X = S or Se, are indirect semiconductors.[16] With the decreasing of the layers, TMDCs will change from indirect semiconductors into direct semiconductors.[17,18] Monolayer MoS$_2$ has a direct band gap ~1.90 eV in the visible frequency range. It has strong Rashba spin-orbit interaction (RSOI), which is responsible for a wide variety of novel physical phenomena.[14,19–26] It is well known that the Rashba effect can be induced by breaking of inversion symmetry. Introducing external electric field is a natural way to break this symmetry and induce a strong Rashba effect based on the relation $H_{Rashba} = -\frac{e\hbar}{4m_e^2c^2}\hat{\sigma}\cdot(\nabla V(\mathbf{r})\times\mathbf{p})$, where $\hat{\sigma}$ is the Pauli matrix, $V(\mathbf{r})$ is the electronic potential, and $\mathbf{p}$ is the carrier momentum.

Due to the Rashba effect, an electron moving with a momentum $\mathbf{p}$ in the electric field can feel an effective magnetic field $\mathbf{B}_{eff} \equiv \nabla V(\mathbf{r})\times\mathbf{p}/2mc^2$. For monolayer MoS$_2$, there are intrinsic internal electric dipole fields in the monolayer plane which give perpendicular effective magnetic fields and cause Zeeman-like spin up/down texture in most region of

momentum space.[14,15] Once an external electric field $\mathbf{E}_{ext}$ perpendicular to the monolayer plane is turned on, an extra effective magnetic field will orient the spin toward the plane and an extra spin precession will be induced. As H_{Rashba} is proportional to the strength of the electric field, the spin can be manipulated by $\mathbf{E}_{ext}$. Recently, Gong *et al.*[27] have studied the transport properties of WSe$_2$ based field effect transistor (FET) and concluded that the transmission probability for a carrier passing through such a FET depends critically on whether the electron spin orientation is matched to the spin orientations in the drain contact or not. In this paper, we will study the conductance of MoS$_2$ based nano-devices from first principles as a function of the voltage of the gate and the length of the gate in the scattering region. Oscillatory behaviors for conductance were found which can be attributed to spin precession of electron in the effective magnetic field due to the gate voltage.

II. COMPUTATION DETAILS

As shown in Fig. 1, our device consists of a central scattering region coupled to source and drain which extends to $y = -\infty$ and $y = +\infty$ where bias voltage is applied and current is collected. The potential of the central region is controlled by bottom gate voltage V_g. The transport is in y direction, which is along zigzag direction. Periodic boundary condition is satisfied in x direction. In the numerical calculation, the size of central scattering region is set as $10.34a_B \times 47.77a_B \times 26.35a_B$ including a vacuum of

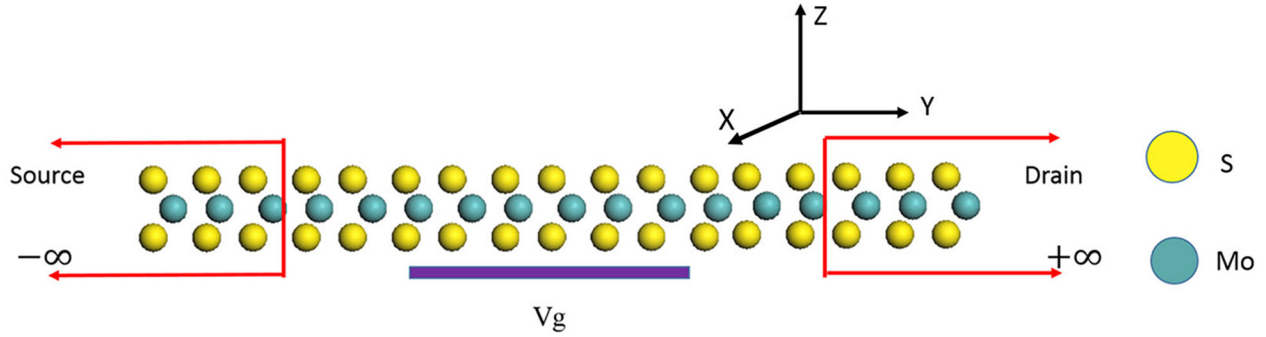a)Authors to whom correspondence should be addressed. Electronic addresses: ywei@szu.edu.cn and jianwang@hku.hk

117, 104307-1

FIG. 1. Structure of monolayer MoS$_2$ field effect transistor with a bottom gate (side view). Source and drain extend to $y = -\infty$ and $y = +\infty$. Mo and S atoms are shown in cyan and yellow.

thickness $20.36a_B$ along z direction. In the calculation, we have used density functional theory (DFT) within the non-equilibrium Green's function (NEGF) formalism[28,29] as implemented in the first principles quantum transport package Nanodcal. SOI, non-collinear spin, and gate potential are all included in our self-consistent calculation. For technical details, we refer interested readers to references.[28–30] In the self-consistent calculation, the generalized gradient approximation (GGA) is used as the exchange-correlation functional,[31] the standard norm-conserving nonlocal pseudo-potentials as the atomic core,[32] and a linear combination of double-ζ atomic orbital as the basis.[28] We have used bulk values for the structure constants because the crystal structure of isolated MoS$_2$ layers remain to be the same as stacked layers within bulk crystals.[16] We note that for the monolayer TMDC, due to the strong spin-orbital interaction, spin is not a good quantum number. Hence, it is a non-collinear spin self-consistent calculation which is very time consuming.

To analyze the spin behavior in the presence of gate voltage, we follow Ref. 33 to define a spin polarization vector $\mathbf{P} = (P_x, P_y, P_z)$, which is obtained by decomposing the charge Q_{nk} using the Pauli matrix σ, $Q_{nk} = Q\mathbf{I} + P_x\sigma_x + P_y\sigma_y + P_z\sigma_z$. Here, n is the band index, k is the wave vector, and $\mathbf{I}$ is the unit matrix. Then the tilting angle $\Phi(\mathbf{r}) = arc\tan[P_z/(P_x^2 + P_y^2)^{1/2}]$ is used to identify the spin texture. One can, of course, define the total spin tilting angle Φ by averaging spin polarization vector first then calculating tilting angle. When spin is polarized along the z-direction,

i.e., perpendicular to the 2D plane, we will have $\Phi = 90°$ for spin up and $\Phi = -90°$ for spin down.

III. RESULTS AND DISCUSSIONS

Using Nanodcal code,[28–30] we find that the monolayer MoS$_2$ has a direct energy band gap $E_{gap} = 1.73$ eV with the valence band maximum located at K or K' (see Fig. 2 and Table I). Compared with experimental values, our result underestimates the direct gap at $K(K')$ by about 0.2 eV, but the spin splitting $\sim$0.15 eV at the top valence band is in good agreement with experimental value, as shown in Table I. To see the spin texture around K or K' clearly, we plot energy band along the first Brillouin zone edge and the corresponding total spin polarization vector Φ of the top two valence bands without gate in Fig. 3. The red valance band (see K_{v1} in Fig. 2) has $\Phi = 90°$ near K and $\Phi = -90°$ near K', while the black valance band (see K_{v2} in Fig. 2) has $\Phi = 90°$ near K' and $\Phi = -90°$ near K. This indicates that the spin texture is Zeeman-like and the spins are locked with valley index.

Next, we discuss the influence of the gate on the electronic transport of monolayer MoS$_2$ FET. We focus on the spin transport in the energy range -0.85 to -0.70 eV near the top of valence band, where the Zeeman-like spin splitting occurs and electrons either pass through K_{v1} near K (spin up electrons) or near K' (spin down electrons). Fig. 4(a) gives the conductance as a function of gate voltage at three different Fermi energies with the gate length $L_0 = 22.89a_B$. Fig. 4(b) gives the conductance as a function of the gate length with a fixed gate voltage $V_g = -3.0$ V. One finds that conductance oscillates with both the gate voltage V_g and with the gate length L. In Fig. 4(a), the maximum conductance happens at about $V_g = -1.6$ V or $V_g = -3.8$ V, while the minimum conductance appears at about $V_g = -2.8$ V and $V_g = -5.0$ V.
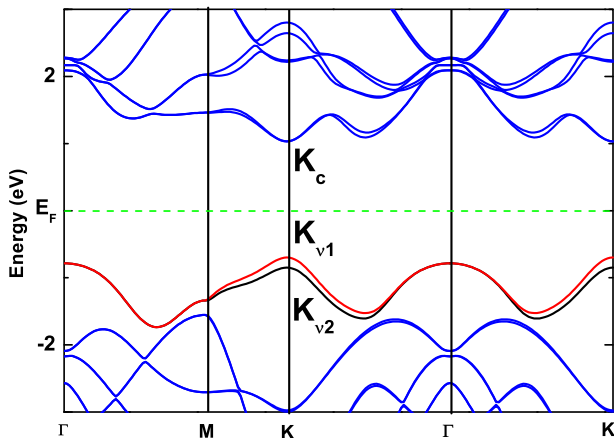

FIG. 2. Electronic band structure of the monolayer MoS$_2$. The Fermi level is indicated by the horizontal dashed green line.

TABLE I. Interband transitions near K in monolayer MoS$_2$.

Transitions	Transition energy (eV)		
	Calculated	Previous calculation[34]	Experiment
K_{v1} to K_c	1.73	1.60–2.82	1.90[a]
K_{v2} to K_{v1}	0.15	0.146–0.193	0.10[b]

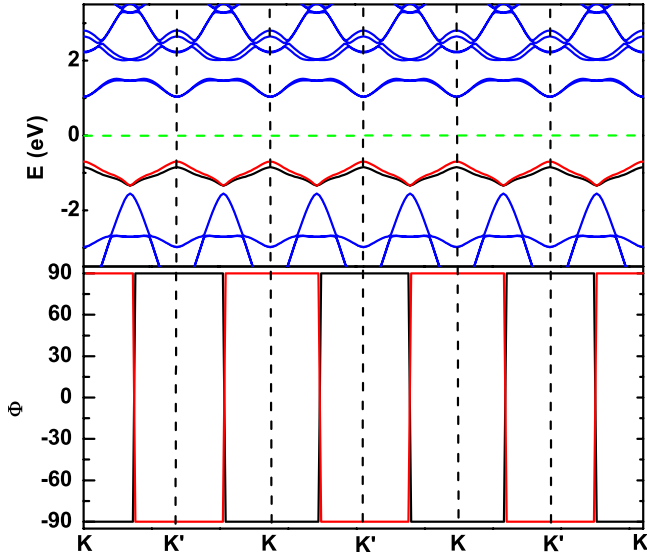[a]Reference 9.
[b]Reference 35.

FIG. 3. Energy band (upper panel) and total tilting angle Φ (lower panel) along the edge of the first Brillouin zone for the uppermost two spin splitting valence bands. The red and black lines correspond to the two splitting valence bands marked in the same colors in Fig. 2.
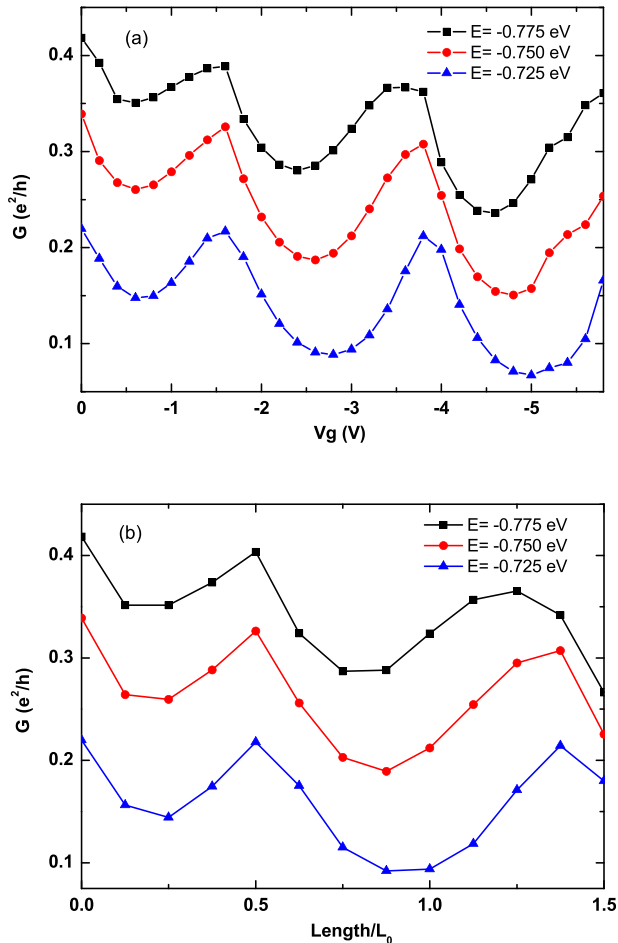

FIG. 4. (a) Conductance G versus the gate voltage V_g for the monolayer MoS$_2$ FET with the length of gate $L = L_0 = 22.89 a_B$; (b) G versus the length of gate at $V_g = -3.0$ V. a_B is Bohr radius.

To understand the oscillatory behavior, we calculate the spin polarization vector **P** at the energy $E = -0.725$ eV and the spin tilting angles in real space. In Fig. 5, we plot the spin tilting angle $\Phi(y)$, which is averaged over x in xy-plane,[36] as a function of y-position along the scattering region at several different gate voltages V_g near K' valley. To see the effect of the gate voltage clearly, we perform fast Fourier transform (FFT) filter using 25 points on the original data to smooth the curves (see the red dashed lines in Fig. 5). As mentioned earlier, the spin texture is almost Zeeman-like with $\Phi(y)$ close to $-90°$ [see Fig. 5(a)] when $V_g = 0.0$ V. The small departure from $-90°$ in real space comes from the intrinsic spin precession due to internal electric field among S and Mo atoms. If we average the spin polarization vector **P** over all scattering region and then calculate the tilting angle, we will get $\Phi = -90°$. From Fig. 5(a), we find that the tilting angle shows small quick oscillation in real space, and the oscillation period along the transport direction is almost half length of the y-coordinate difference between the nearest neighbor Mo and S atoms. The quick oscillation in Fig. 5(a) implies that the internal electric field is very strong.[15] When V_g is turned on, an external electric field in the z-direction is added. It is perpendicular to the internal electric field which is in the xy-plane. So additional spin precession due to RSOI caused by the gate voltage will appear. Compared with the strength of internal electric field,[15] the strength of the gate electric field felt by MoS$_2$ is much smaller giving rise to a much slower spin precession. It can be observed from Figs. 5(b)–5(e) that for $V_g = -1.6$ V or -3.8 V, $\Phi(y)$ returns to its initial state of entering the scattering region when the electron leaves the scattering region, resulting a conductance peak. While for $V_g = -2.8$ V or -5.0 V, $\Phi(y)$ has obvious departure from its initial state after electron traversing
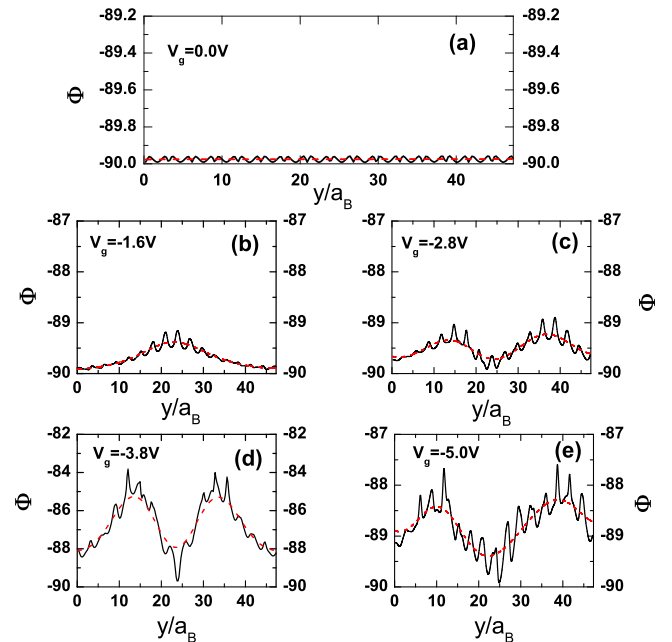

FIG. 5. Tilting angle Φ averaged over x in xy-plane along the transport y-direction (the zigzag direction) for (a) $V_g = 0.0$ V, (b) $V_g = -1.6$ V, (c) $V_g = -2.8$ V, (d) $V_g = -3.8$ V, and (e) $V_g = -5.0$ V. a_B is Bohr radius. The red dashed lines are smoothed tilting angle obtained by 25 points fast Fourier transform filter on the original data (black lines).

through the scattering region and the electron conductance reaches its minimum.

Such spin transport cross the central region can also be understood by the concept of spin precessing along a magnetic field.[37] We suppose that the electron has an initial spin with polar angles θ and ϕ in spherical coordinate. In σ_z representation, the state of the electron would be $|\psi\rangle = |\uparrow\rangle a_1 + |\downarrow\rangle a_2$, where $a_1 = \cos\frac{\theta}{2}e^{-i\phi/2}$, $a_2 = \sin\frac{\theta}{2}e^{+i\phi/2}$, and $|\uparrow\rangle, |\downarrow\rangle$ are the eigen states of $s_z = \pm\frac{\hbar}{2}$. When a magnetic field B in z-direction is turned on, the states of the electron can be obtained from the Schrödinger equation $i\hbar\frac{\partial\psi}{\partial t} = \hat{H}\psi$ with the Hamiltonian $H = -\mu_B B\sigma_z$, where μ_B is the Bohr magneton. Then $|\psi(t)\rangle = |\uparrow\rangle a_1 e^{+i\mu_B Bt/\hbar} + |\downarrow\rangle a_2 e^{-i\mu_B Bt/\hbar}$. After a period T, the angle ϕ is changed by $2u_B BT/\hbar$ and the angle θ is unchanged. The quantum mechanical results of the spin direction variation can be viewed as that one just rotates the spin direction around the axis of B with the vector angular velocity $\omega = 2\mu_B B/\hbar$.

In our FET, the external gate V_g gives rise to an effective magnetic field B_{eff} pointing to the direction according the resultant electric field. When the electron reaches the gated region, its spin starts to process along the effective B_{eff} until leaving the gate region. Because the angular velocity $\omega = 2\mu_B B_{eff}/\hbar$ depends on the B_{eff}, or V_g, for a fixed length of gated region, the precessing angle of the spin depends on the value of V_g. As shown in Figs. 5(b) and 5(d), after the spin precessing in the gate region, the spin polarization tilting angle $\Phi(y)$ in the drain side matches with $\Phi(y)$ in the source side, which is responsible for the maxima conductance in Fig. 4(a) for $E = -0.725$ eV. However, in Figs. 5(c) and 5(e), a large deviation occurs between the spin polarization tilting angles $\Phi(y)$ in source and drain. In this situation, the conductance is small and reaches its minima in Fig. 4(a). On the other hand, the length of the gated region along the y direction determines the time of the spin precession, therefore the number of complete precession cycle. Thus, the transport of the spin can also be modulated periodically by the length of the gate, as shown in Fig. 4(b).

IV. CONCLUSIONS

In summary, using DFT within the framework of NEGF, the behavior of electron through a monolayer MoS_2 FET is investigated from first principles. The Rashba effect due to external electric field on the transport properties is examined. Our first principle calculations show that with a fixed length of gated region, the conductance of electron oscillates with V_g. On the other hand, once V_g is fixed, the conductance also shows an oscillatory behavior with the length of gated region. Such interesting behaviors of electron modulated by the external electric field can be well understood by the dynamics of electron in the effective magnetic field.

ACKNOWLEDGMENTS

[1]K. S. Novoselov, A. K. Geim, S. V. Morozov, D. Jiang, Y. Zhang, S. V. Dubonos, I. V. Grigorieva, and A. A. Firsov, Science **306**, 666 (2004).

[2]K. S. Novoselov, A. K. Geim, S. V. Morozov, D. Jiang, M. I. Katsnelson, I. V. Grigorieva, S. V. Dubonos, and A. A. Firsov, Nature (London) **438**, 197 (2005).

[3]Y. Zhang, Y. W. Tan, H. L. Stormer, and P. Kim, Nature(London) **438**, 201 (2005).

[4]S. B. Fagan, R. J. Baierle, R. Mota, Z. J. R. da Silva, and A. Fazzio, Phys. Rev. B **61**, 9994 (2000).

[5]S. Lebègue and O. Eriksson, Phys. Rev. B **79**, 115409 (2009).

[6]S. Cahangirov, M. Topsakal, E. Aktürk, H. Şahin, and S. Ciraci, Phys. Rev. Lett. **102**, 236804 (2009).

[7]A. Splendiani, L. Sun, Y. Zhang, T. Li, J. Kim, C. Y. Chim, G. Galli, and F. Wang, Nano Lett. **10**, 1271 (2010).

[8]A. Ayari, E. Cobas, O. Ogundadegbe, and M. S. Fuhrer, J. Appl. Phys. **101**, 014507 (2007).

[9]K. F. Mak, C. Lee, J. Hone, J. Shan, and T. F. Heinz, Phys. Rev. Lett. **105**, 136805 (2010).

[10]B. Radisavljevic, A. Radenovic, J. Brivio, V. Giacometti, and A. Kis, Nat. Nanotechnol. **6**, 147 (2011).

[11]H. Zeng, J. Dai, W. Yao, D. Xiao, and X. Cui, Nat. Nanotechnol. **7**, 490 (2012).

[12]K. F. Mak, K. He, J. Shan, and T. F. Heinz, Nat. Nanotechnol. **7**, 494 (2012).

[13]T. Cao, G. Wang, W. P. Han, H. Q. Ye, C. R. Zhu, J. R. Shi, Q. Niu, P. H. Tan, E. G. Wang, B. L. Liu, and J. Feng, Nat. Commun. **3**, 887 (2012).

[14]D. Xiao, G. B. Liu, W. Feng, X. Xu, and W. Yao, Phys. Rev. Lett. **108**, 196802 (2012).

[15]H. Yuan, M. S. Bahramy, K. Morimoto, S. Wu, K. Nomura, B. J. Yang, H. Shimotani, R. Suzuki, M. Toh, C. Kloc, X. Xu, R. Arita, N. Nagaosa, and Y. Iwasa, Nat. Phys **9**, 563 (2013).

[16]Th. Böker, R. Severin, A. Müller, C. Janowitz, R. Manzke, D. Voß, P. Krüger, A. Mazur, and J. Pollmann, Phys. Rev. B **64**, 235305 (2001).

[17]T. Cheiwchanchamnangij and W. R. L. Lambrecht, Phys. Rev. B **85**, 205302 (2012).

[18]S. W. Han, H. Kwon, S. K. Kim, S. Ryu, W. S. Yun, D. H. Kim, J. H. Hwang, J. S. Kang, J. Baik, H. J. Shin, and S. C. Hong, Phys. Rev. B **84**, 045409 (2011).

[19]Z. Y. Zhu, Y. C. Cheng, and U. Schwingenschlögl, Phys. Rev. B **84**, 153402 (2011).

[20]I. Žutić, J. Fabian, and S. D. Sarma, Rev. Mod. Phys. **76**, 323 (2004).

[21]S. Murakami, N. Nagaosa, and S. C. Zhang, Science **301**, 1348 (2003).

[22]J. Sinova, D. Culcer, Q. Niu, N. A. Sinitsyn, T. Jungwirth, and A. H. MacDonald, Phys. Rev. Lett. **92**, 126603 (2004).

[23]S. Q. Shen, M. Ma, X. C. Xie, and F. C. Zhang, Phys. Rev. Lett. **92**, 256603 (2004).

[24]D. Culcer, J. Sinova, N. A. Sinitsyn, T. Jungwirth, A. H. MacDonald, and Q. Niu, Phys. Rev. Lett. **93**, 046602 (2004).

[25]E. I. Rashba and Al. L. Efros, Phys. Rev. Lett. **91**, 126405 (2003).

[26]Q. F. Sun, J. Wang, and H. Guo, Phys. Rev. B **71**, 165310 (2005).

[27]K. Gong, L. Zhang, D. Liu, L. Liu, Y. Zhu, Y. Zhao, and H. Guo, Nanotechnology **25**, 435201 (2014).

[28]J. Taylor, H. Guo, and J. Wang, Phys. Rev. B **63**, 245407 (2001).

[29]D. Waldron, P. Haney, B. Larade, A. MacDonald, and H. Guo, Phys. Rev. Lett. **96**, 166804 (2006).

[30]See http://www.nanoacademic.ca for details of the NanoDcal quantum transport package.

[31]J. P. Perdew, K. Burke, and M. Ernzerhof, Phys. Rev. Lett. **77**, 3865 (1996).

[32]D. R. Hamann, M. Schlüter, and C. Chiang, Phys. Rev. Lett. **43**, 1494 (1979).

[33]Y. Zhao, Y. Hu, L. Liu, Y. Zhu, and H. Guo, Nano Lett. **11**, 2088 (2011).

[34]A. Ramasubramaniam, Phys. Rev. B **86**, 115409 (2012).

[35]L. F. Sun, J. X. Yan, D. Zhan, L. Liu, H. L. Hu, H. Li, B. K. Tay, J.-L. Kuo, C.-C. Huang, D. W. Hewak, P. S. Lee, and Z. X. Shen, Phys. Rev. Lett. **111**, 126801 (2013).

[36]We averaged the spin polarization vector **P** first in *xy*-plane with $z = 0$, then calculate tilting angles.

[37]R. Feynman, R. B. Leighton, and M. L. Sands, *The Feynman Lectures on Physics* (Addison-Wesley Publishing Company, Boston), 2004, Vol. 3.